Journal of Solid State Chemistry **166,** 434–441 (2002)
doi:10.1006/jssc.2002.9625

A Neutron Diffraction Study of the Thermal Stability of the α-Quartz-Type Structure in Germanium Dioxide

J. Haines,*[,1] O. Cambon,* E. Philippot,* L. Chapon,† and S. Hull‡

*Laboratoire de Physicochimie de la Matière Condensée, UMR CNRS 5617, Université Montpellier II, cc 003, Place E. Bataillon, 34095 Montpellier Cedex 5, France; †Argonne National Laboratory, Materials Science Division 223, 9700 South Cass Avenue, Argonne, Illinois 60439; and ‡Rutherford Appleton Laboratory, ISIS Science Division, Chilton, Didcot, Oxfordshire, OX11 0QX, United Kingdom

Received January 23, 2002; in revised form April 5, 2002; accepted April 19, 2002

The structure of the α-quartz-type form of germanium dioxide was refined at room temperature and up to 1344 K by the Rietveld method using time-of-flight neutron powder diffraction data. The intertetrahedral bridging angle θ and the tilt angle δ exhibit thermal stabilities that are among the highest observed in α-quartz homeotypes. The temperature dependence of these angles is found to be a function of the structural distortion in these materials. Structure–property relationships predict that due to its highly distorted structure, germanium dioxide is potentially a high-performance piezoelectric material. The high stability of the above structural parameters as a function of temperature infers that the corresponding piezoelectric properties should also be retained under these conditions. At the present time, problems related to phase stability and crystal growth need to be resolved before the α-quartz-type form of germanium dioxide can be used as a piezoelectric material. © 2002 Elsevier Science (USA)

Key Words: **germanium dioxide; quartz; piezoelectricity; neutron diffraction; crystal structure; high temperature.**

INTRODUCTION

α-Quartz is the most used piezoelectric material at the present time. However, its performances are too limited for certain technological applications, particularly in microelectronic components such as frequency filters and resonators requiring high frequencies and consequently miniaturization. This has spurred research into finding analogous materials with better intrinsic properties. Structure–property relationships have been developed for α-quartz and ternary ABO_4 (A = B, Al, Ga, Fe; B= P, As) α-berlinite ($AlPO_4$) isotypes (1–4). The latter structure type corresponds to a cation-ordered derivative of the α-quartz type with a doubled **c** parameter. In both cases, the space group is $P3_121$ (or $P3_221$) with $Z = 3$. The piezoelectric coupling coefficient of these materials was found to increase linearly as a function of structural distortion with respect to β-quartz structure type. This distortion can be described in terms of the intertetrahedral A–O–B bridging angle, θ, or the tilt angle with respect to the β-quartz structure type, δ (note for β-quartz $\theta = 154°$, $\delta = 0°$)· The most distorted structures found among α-quartz homeotypes (3,5) are those of GeO_2 ($\theta = 130.0°$, $\delta = 26.6°$) and $GaAsO_4$ ($\theta = 129.6°$, $\delta = 26.9°$). Based on structure-property relationships, these compounds should exhibit the highest piezoelectric coupling coefficients for α-quartz-type materials.

An important property of a piezoelectric material from the point of view of potential applications is its thermal stability. The temperature domain of application of α-quartz, for example, is limited by the $\alpha-\beta$ phase transition at 846 K (6) and the consequent loss of piezoelectric properties. The $\alpha-\beta$ phase transition temperature was found to increase as a function of the structural distortion in these materials (1) and for values of $\theta < 136°$ and $\delta > 22°$; the $\alpha-\beta$ phase transition is absent. In view of its distorted structure, germanium dioxide should be one of the best potential piezoelectric materials of the α-quartz type. It is, thus, very important to determine the temperature dependence of the angles θ and δ as the piezoelectric properties of the material are related to the values of these angles and the smaller the variation with temperature the more stable these properties will be.

Under ambient conditions, germanium dioxide is stable in the rutile form in which germanium is in six-fold coordination. The transition to the α-quartz-type form begins at close to 1310 K followed by fusion at 1389 K (7). This polymorph is metastable under ambient conditions and can be obtained by cooling from above 1310 K and from direct synthesis from various precursors, such as by the hydrolysis of $GeCl_4$ (8). Crystal growth of this

[1] To whom correspondence should be addressed. Fax: +33-467144290. E-mail: jhaines@lpmc.univ-montp2.fr.

0022-4596/02 $35.00

metastable form is currently an important subject of investigation and the preparation of large, single crystals is difficult (9). Up to the present, the structural stability of this form at high temperature has only been studied by X-ray powder diffraction (3); however, the low relative X-ray scattering factor of oxygen with respect to germanium severely limits the precision of such measurements. This is not the case for neutron diffraction, for which the scattering values are of a comparable magnitude. The structure of this material and the effect of temperature can best be determined using neutron diffraction data. We have thus used neutron powder diffraction data to refine the structure of the α-quartz form of GeO_2 as a function of temperature up to within 10° of the melting point. The results will allow us to further develop the structure–property relationships in these materials.

EXPERIMENTAL

Germanium dioxide was studied at two different neutron sources. Time-of-flight (TOF) neutron diffraction data were obtained on the Polaris medium resolution diffractometer (10) at the ISIS spallation source of the Rutherford Appleton Laboratory and on Special Environment Powder Diffractometer (SEPD) at the IPNS spallation source at the Argonne National Laboratory.

Germanium dioxide powder (5 cm^3) (Produits Touzart & Matignon, purity 99.999%) were used in the experiment at ISIS, which had a phase purity of 99.4% (11) with the remaining 0.6% being in the rutile-type phase. The sample was placed in a 10 mm diameter standard vanadium sample can in the neutron beam. Data were collected over a TOF range from 850 to 19,600 μs ($d = 0.1376-3.1800$ Å) at a diffraction angle $2\theta = 145°$ using a bank of ^{3}He ionization counters. The acquisition time was of the order of 0.5 h. The data were normalized with respect to those of a standard vanadium sample. High-temperature measurements were performed on the same sample in the Rutherford Appleton Laboratory Furnace equipped with vanadium heating elements. The acquisition time for the high-temperature runs was typically 1–2 h. Temperatures were measured with a thermocouple placed in contact with the vanadium can.

The Argonne data were obtained using 5 cm^3 of GeO_2 powder from Strem (purity 99.999%) with a rutile-phase content of 1.2%. Data were collected over a TOF range from 2500 to 29,495 μs ($d = 0.3346-3.9487$ Å) at a diffraction angle $2\theta = 144.85°$ using a bank of ^{3}He ionization counters. The high-temperature data were obtained using a Howe furnace and temperatures were measured with a thermocouple as above. The acquisition times were of the order of 1 h.

The data were converted from variable-step format to fixed-step format for use with the Rietveld refinement program GSAS (12). Single-phase refinements were performed for patterns in which the content of the rutile-type phase was less than about 1%; otherwise two-phase refinements were necessary. Refinements were typically performed using the diffraction data (TOF = 2998−16,000 μs; $d = 0.4853-2.5950$ Å) for single phase and TOF = 2998 or 3994–19,600 μs ($d = 0.4853$ or $0.6467-3.1800$ Å) for two phase refinements using data from Polaris. Two phase refinements were performed using the SEPD data (TOF = 3738−29,495 μs; $d = 0.5000-3.9487$ Å). In the refinements, the cell constants, atomic positions, atomic displacement parameters, the scale factor and 2–5 line shape parameters were varied along with up to 24 background parameters to account for background contributions due to diffuse scattering (13). An absorption correction was also applied. The data were first refined using isotropic atomic displacement parameters. Anisotropic atomic displacement parameters were also refined for the data obtained at ambient temperature and the high-temperature data obtained on SEPD. This was possible for the latter as the data were obtained over a larger TOF range. In the case of the ISIS data, refinement of the anisotropic atomic displacement parameters led to unreasonable contraction of the Ge–O distances at high temperature. R_{wp} and R_p agreement factors correspond to the background subtracted values. The large differences in the R_{wp} and χ^2 values between the Polaris and SEPD data are due to differences in the furnace backgrounds and noise levels and the effect of this on the weight and the fit for points at low d-spacings. R_p values are equivalent in both data sets. Figures in parentheses refer to standard deviations obtained directly from the structure refinements

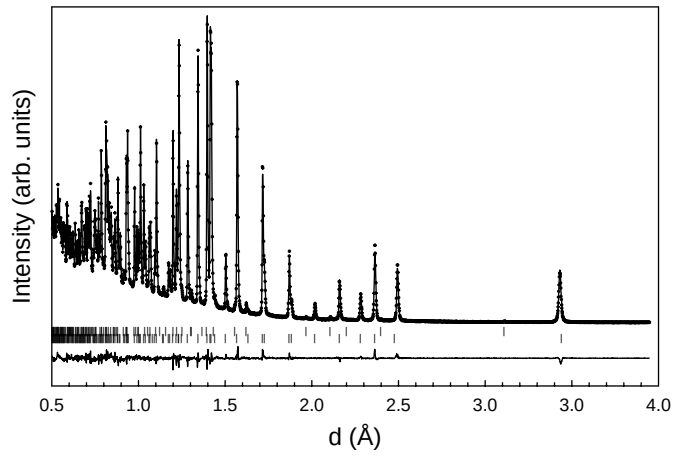

FIG. 1. Experimental data (+), calculated and difference profiles (solid lines) from the Rietveld refinement of α-quartz-type GeO_2 at 298 K using neutron diffraction data from SEPD. Intensity is in arbitrary units and the difference profile is on the same scale. Vertical bars indicate the positions of all calculated reflections for the α-quartz-type phase (below) and the rutile-type phase (above).

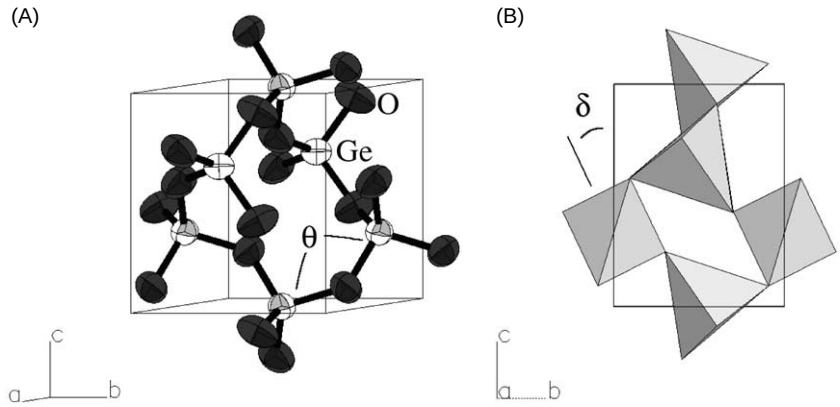

FIG. 2. (A) The crystal structure of α-quartz-type GeO_2 at 298 K. Atomic displacement ellipsoids are plotted at 99.9% probability. (B) Polyhedral representation of the crystal structure of α-quartz-type GeO_2 at 298 K. The angle δ corresponds to the tilt of the GeO_4 tetrahedron about its two-fold axis with respect to its orientation in a hypothetical β-quartz-type structure.

using GSAS. Such values obtained using the Rietveld method are known to underestimate the true uncertainty in refined structural parameters.

RESULTS AND DISCUSSION

Structural Evolution at High Temperature

The results of the Rietveld refinements using neutron diffraction data obtained at ambient temperature (Figs. 1 and 2 and Tables 1–5) are in very good agreement with previous single-crystal X-ray diffraction studies on small crystals (5, 14). In fact, the intertetrahedral Ge–O–Ge bridging angle, θ, and the tilt angle, δ, which are very sensitive to the fractional atomic coordinates agree remarkably well.

Expansion of the unit cell is highly anisotropic, (Table 2 and Fig. 3) with the c/a ratio decreasing from 1.1328 at 294 K to 1.1178 at 1344 K. The thermal expansion coefficient of the α-quartz-type phase (Fig. 3) was found to be $\alpha(K^{-1}) = 3.19 \times 10^{-5} + 9.8 \times 10^{-9}(T - 300)$. This is slightly greater than previous values at 300 K which range from $2.35 \times 10^{-5}\,K^{-1}$ to $2.99 \times 10^{-5}\,K^{-1}$ (15,16). The linear thermal expansion coefficients are $\alpha_a = 1.67 \times 10^{-5}\,K^{-1}$ and $\alpha_c = 3.42 \times 10^{-6}\,K^{-1}$. Thermal expansion of the α-quartz-type structure along **a** is thus five

TABLE 1
Details of Rietveld Refinements

T (K)	Number of reflections[a]	Number of variable parameters	Weight fraction of rutile phase (%)	Agreement factors			
				R_{wp}	R_p	Reduced χ^2	R_{Bragg}[a]
294	489	38	<1	0.017	0.026	2.4	0.033
298	*583*	*53*	*1.2*	*0.041*	*0.028*	*2.1*	*0.037*
425	*582*	*52*	*1.2*	*0.112*	*0.042*	*1.2*	*0.057*
449	494	32	<1	0.026	0.028	7.5	0.053
571	*583*	*52*	*1.4*	*0.137*	*0.045*	*1.2*	*0.078*
634	496	32	<1	0.030	0.031	7.9	0.066
756	*587*	*52*	*1.5*	*0.153*	*0.045*	*1.2*	*0.089*
845	669	38	*1.4*	0.034	0.035	5.8	0.072
890	*585*	*52*	*1.8*	*0.208*	*0.049*	*1.1*	*0.086*
1043	*584*	*48*	*13.6*	*0.221*	*0.056*	*1.2*	*0.118*
1059	666	47	10	0.034	0.038	9.3	0.065
1175	670	45	28.5	0.028	0.040	7.3	0.048
1215[b]	288	40	14	0.042	0.050	3.7	0.069
1275[b]	*368*	*39*	*18.5*	*0.181*	*0.054*	*1.3*	*0.095*
1298	669	38	30.9	0.028	0.035	10.6	0.067
1344	289	29	3.5	0.049	0.058	7.5	0.100

Note. The SEPD data are italicized.
[a] Total = α-quartz-type + rutile-type phases.
[b] Data obtained on cooling.

TABLE 2
Unit Cell Constants and Volume of α-Quartz-Type GeO_2 as a Function of Temperature

T (K)	a (Å)	c (Å)	V (Å^3)
294	4.98503(3)	5.64711(4)	121.532(1)
298	*4.98535(2)*	*5.64503(4)*	*121.503(1)*
425	*4.99462(5)*	*5.64887(9)*	*122.038(3)*
449	4.99508(3)	5.65120(6)	122.111(2)
571	*5.00456(5)*	*5.65283(10)*	*122.610(3)*
634	5.00826(4)	5.65720(8)	122.887(3)
756	*5.01823(6)*	*5.65851(12)*	*123.405(4)*
845	5.02490(4)	5.66238(8)	123.818(3)
890	*5.02861(7)*	*5.66227(13)*	*123.998(5)*
1043	*5.04558(6)*	*5.66088(11)*	*124.806(4)*
1059	5.04571(3)	5.66230(6)	124.844(2)
1175	5.05580(3)	5.66433(6)	125.388(2)
1215[a]	5.05734(5)	5.66450(9)	125.469(3)
1275[a]	*5.06802(6)*	*5.66645(12)*	*126.042(4)*
1298	5.06649(4)	5.66670(8)	125.972(3)
1344	5.07022(5)	5.66741(9)	126.173(3)

[a] Data obtained on cooling.

times that along **c** (see below). The thermal expansion of GeO_2 is lower than that of SiO_2 for which the value of α is $3.53 \times 10^{-5}\,K^{-1}$ (17).

Intratetrahedral distances and angles are relatively stable as a function of temperature (Table 5). There is a slight tendency for the Ge–O distances to *decrease* as a function of temperature. Similar, apparently, non-physical behavior has been observed for all α-quartz homeotypes (3,13, 18–24). In the case of α-quartz, this has been shown (13) to be due to dynamic disorder in the structure, which is accommodated by a reduction in the time-averaged Si–O distances. The total neutron scattering data indicate that the instantaneous Si–O distance increases with temperature as would be expected.

The relative stability of the intratetrahedral distances and angles would imply that the observed thermal expansion arises mainly from the increase in the intertetrahedral Ge–O–Ge bridging angle, θ and from tilting of the GeO_4 tetrahedra. The intertetrahedral Ge–O–Ge bridging angle, θ, and the tilt angle, δ, were found to increase and decrease respectively as a function of temperature, (Table 5 and Figs. 4 and 5). The tilt angle δ (Fig. 2), is an order parameter for the $\alpha-\beta$ phase transition in quartz-type materials (25). It can be seen that even at 10° below the melting point, the α-quartz-type structure remains highly distorted ($\delta = 23.7°$) with respect to the β-quartz structure type ($\delta = 0°$). The value of θ, 133.7°, is also significantly less than 154°, the value corresponding to the β-quartz structure type. The increase in θ and the decrease in the tilt angle δ contribute strongly to expansion in the xy plane (Fig. 2) leading to the strongly anisotropic thermal expansion observed.

Thermal Stability of α-Quartz-Type Structures

The temperature dependence of the intertetrahedral A–O–A' bridging angle, θ, and the tilt angle, δ, is lower than those of all α-quartz homeotypes (18–24), except gallium arsenate (3), for which the values are similar. The latter is also highly distorted with θ and δ values which are,

TABLE 3
Fractional Atomic Coordinates and Isotropic or Equivalent[a] Atomic Displacement Parameters for α-Quartz-Type GeO_2 as a Function of Temperature

T (K)	x_{Ge}	$100 \times U_{iso}$ or U_{eq}	x_O	y_O	z_O	$100 \times U_{iso}$ or U_{eq}
294	0.4511(1)	0.57(1)	0.3974(1)	0.3022(1)	0.2425(1)	1.07(2)
298	*0.4512(1)*	*0.87(2)*	*0.3971(2)*	*0.3023(1)*	*0.2428(1)*	*1.67(4)*
425	*0.4527(3)*	*1.19 (6)*	*0.3970(4)*	*0.3009(3)*	*0.2418(2)*	*2.01(8)*
449	0.4517(1)	0.97(1)	0.3995(2)	0.3019(2)	0.2431(2)	1.67(1)
571	*0.4530(3)*	*1.65 (8)*	*0.3976(4)*	*0.2996(4)*	*0.2412(3)*	*2.50(9)*
634	0.4531(2)	1.45(2)	0.4000(2)	0.3003(2)	0.2422(2)	2.45(2)
756	*0.4543(4)*	*2.06 (10)*	*0.3983(5)*	*0.2977(5)*	*0.2400(3)*	*3.25(12)*
845	0.4545(2)	1.95(2)	0.4006(3)	0.2984(2)	0.2409(2)	3.26(2)
890	*0.4555(4)*	*1.81 (12)*	*0.3988(7)*	*0.2957(6)*	*0.2386(4)*	*3.31(16)*
1043	*0.4572(6)*	*2.10 (15)*	*0.3994(9)*	*0.2937(7)*	*0.2378(5)*	*3.69(20)*
1059	0.4559(2)	2.37(2)	0.3998(3)	0.2949(3)	0.2386(2)	4.10(3)
1175	0.4572(2)	2.59(2)	0.3993(4)	0.2922(3)	0.2373(2)	4.48(4)
1215[b]	0.4572(3)	2.63(3)	0.3985(5)	0.2907(4)	0.2362(3)	4.50(6)
1275[b]	*0.4588(6)*	*2.98 (21)*	*0.3981(11)*	*0.2887(8)*	*0.2357(6)*	*5.28(29)*
1298	0.4583(3)	2.79(3)	0.3998(5)	0.2892(4)	0.2360(3)	4.99(6)
1344	0.4589(2)	2.95(3)	0.3990(5)	0.2880(4)	0.2346(3)	4.93(6)

Note. Space group $P3_121$, $Z = 3$, Ge on 3a sites (x,0,1/3), O on 6c sites (x,y,z).
[a] $U_{eq} = \frac{1}{3}\,[U_{11} + U_{22} + U_{33}]$.
[b] Data obtained on cooling.

TABLE 4
Anisotropic Atomic Displacement Parameters (Å^2) for α-Quartz-Type GeO_2 as a Function of Temperature

T (K)	$100 \times U_{11}$ Ge	$100 \times U_{22}$ Ge	$100 \times U_{33}$ Ge	$100 \times U_{23}$ Ge	$100 \times U_{11}$ O	$100 \times U_{22}$ O	$100 \times U_{33}$ O	$100 \times U_{12}$ O	$100 \times U_{13}$ O	$100 \times U_{23}$ O
294	0.63(1)	0.63(2)	0.46(1)	-0.04(1)	1.55(2)	1.09(2)	0.93(1)	0.93(1)	0.43(1)	0.40(1)
298	*0.88(2)*	*0.69(3)*	*0.70(2)*	*0.00(2)*	*1.67(4)*	*1.36(3)*	*1.07(3)*	*1.03(2)*	*0.39(3)*	*0.35(2)*
425	*1.29(5)*	*1.12(6)*	*1.10(5)*	*0.14(6)*	*2.8(1)*	*2.25(7)*	*1.63(6)*	*1.75(7)*	*0.74(6)*	*0.55(5)*
571	*1.86(6)*	*1.51(8)*	*1.46(7)*	*0.05(7)*	*3.3(1)*	*2.72(8)*	*2.22(8)*	*2.06(8)*	*0.94(8)*	*0.77(6)*
756	*2.27(8)*	*1.8(1)*	*2.0(1)*	*0.1(1)*	*4.3(2)*	*3.6(1)*	*2.8(1)*	*2.7(1)*	*1.4(1)*	*1.28(8)*
890	*2.1(1)*	*1.5(1)*	*1.6(1)*	*0.1(1)*	*4.8(2)*	*3.6(1)*	*2.8(1)*	*3.1(1)*	*1.4(1)*	*1.48(9)*
1043	*2.4(1)*	*2.0(2)*	*1.8(2)*	*0.1(2)*	*5.1(3)*	*3.9(2)*	*3.4(2)*	*3.3(2)*	*2.1(2)*	*1.9(1)*
1275[a]	*2.7(2)*	*3.2(2)*	*3.3(2)*	*0.3(2)*	*7.9(4)*	*5.7(2)*	*4.3(3)*	*4.9(3)*	*2.6(2)*	*2.5(2)*

[a] Data obtained on cooling.

respectively, slightly lower and slightly higher than those of GeO_2 (note: The values of θ and δ given for ternary ABO_4 α-quartz homeotypes are averages of the two distinct values of each in the crystal structures of these materials). In addition, for the more distorted structures no transition to a β-quartz-type structure is observed. The thermal stability of these structural parameters is found to strongly depend on the degree of structural distortion (Figs. 6 and 7). The structural distortion is a measure of the deviation from the β-quartz-type structure and such behavior with respect to temperature, particularly in the case of the tilt angle, which is the order parameter for the $\alpha-\beta$ transition, is in agreement with a Landau-type model (25). That is, the further the material is from the actual or extrapolated temperature for a transition to a β-quartz-type structure, the slower these angles will vary with temperature. The most distorted materials GeO_2 and $GaAsO_4$ exhibit the smallest temperature dependence for the above angles. The temperature dependences of θ and δ (i.e., $1/\theta\ \partial\theta/\partial T$ and $1/\delta\ \partial\delta/\partial T$ obtained from the linear slope over the temperature range including 300 K) are lower by more than a factor of two or four, respectively, compared to the least distorted materials, quartz and berlinite (Figs. 6 and 7). This high thermal stability is particularly attractive from a materials point of view as the piezoelectric properties can also be expected to be much more stable. It can be noted that from extrapolation, the piezoelectric properties of these materials at room temperature are already expected to be greatly superior to those of the other α-quartz homeotypes. The piezoelectric coupling coefficient

TABLE 5
Selected Bond Distances and Angles for α-Quartz-Type GeO_2 as a Function of Temperature

	Bond length (Å)		O–Ge–O angles (deg)					
T (K)	Ge–O_1	Ge–O_2	O_1–Ge–O_2	O_1–Ge–O_2	O_1–Ge–O_1	O_2–Ge–O_2	θ (Ge–O–Ge) Angle (deg)	δ angle (deg)
294	1.7341(4)	1.7405(4)	112.99(3)	106.30(1)	107.88(3)	110.48(4)	130.22(2)	26.53(5)
298	*1.7357(6)*	*1.7407(6)*	*113.04(4)*	*106.32(2)*	*107.72(6)*	*110.49(5)*	*130.05(4)*	*26.61(4)*
425	*1.738(1)*	*1.738(1)*	*113.1(1)*	*106.4(1)*	*107.4(1)*	*110.5(1)*	*130.3(1)*	*26.3(1)*
449	1.731(1)	1.743(1)	112.4(1)	106.4(1)	108.2(1)	111.0(1)	130.6(1)	26.6(1)
571	*1.736(2)*	*1.739(2)*	*113.0(1)*	*106.6(1)*	*107.5(2)*	*110.4(1)*	*130.8(1)*	*26.0(1)*
634	1.732(1)	1.742(1)	112.4(1)	106.6(1)	108.0(1)	111.1(1)	131.0(1)	26.2(1)
756	*1.735(2)*	*1.737(2)*	*112.9(1)*	*106.7(1)*	*107.3(2)*	*110.4(2)*	*131.3(1)*	*25.6(1)*
845	1.732(1)	1.740(1)	112.3(1)	106.7(1)	107.8(1)	111.1(1)	131.6(1)	25.7(1)
890	*1.733(2)*	*1.735(2)*	*112.8(2)*	*106.9(1)*	*107.2(2)*	*110.3(2)*	*131.9(1)*	*25.1(2)*
1043	*1.734(3)*	*1.734(3)*	*112.7(2)*	*107.2(1)*	*106.9(3)*	*110.3(3)*	*132.4(2)*	*24.8(2)*
1059	1.733(1)	1.738(1)	112.5(1)	107.1(1)	107.3(1)	110.3(1)	132.3(1)	25.0(1)
1175	1.731(1)	1.738(1)	112.7(1)	107.3(1)	106.9(1)	110.0(1)	132.7(1)	24.6(1)
1215[a]	1.729(2)	1.737(2)	112.9(1)	107.4(1)	106.7(2)	109.5(2)	133.0(1)	24.3(1)
1275[a]	*1.730(3)*	*1.738(3)*	*113.0(2)*	*107.7(1)*	*106.1(4)*	*109.5(3)*	*133.1(3)*	*24.1(2)*
1298	1.725(2)	1.738(2)	112.6(1)	107.6(1)	106.7(2)	109.8(2)	133.5(1)	24.1(1)
1344	1.727(2)	1.735(2)	112.9(1)	107.7(1)	106.4(2)	109.4(2)	133.7(1)	23.7(1)

[a] data obtained on cooling.

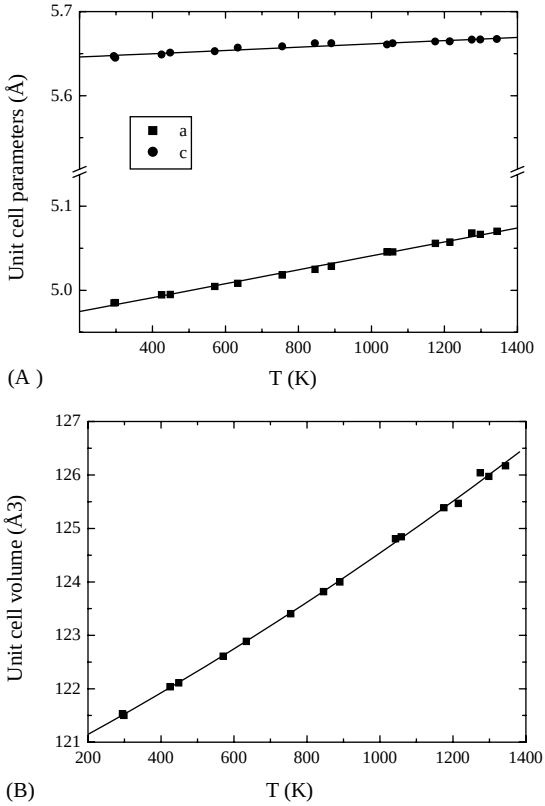

FIG. 3. Unit cell parameters (A) and volume (B) of α-quartz-type GeO_2 as a function of temperature. Solid lines represent linear least-squares fits to the data. The error bars are smaller than the symbol size.

k for the AT cut (a cut for which the resonance frequency is temperature independent) is expected to be about 21% for these two materials as compared to 17% for $GaPO_4$ and only 8.5% for α-quartz (2,3).

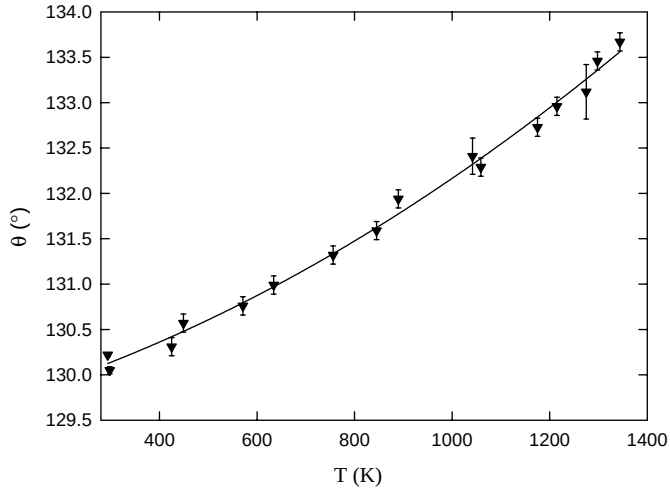

FIG. 4. Evolution of the intertetrahedral bridging angle θ as a function of temperature for α-quartz-type GeO_2.

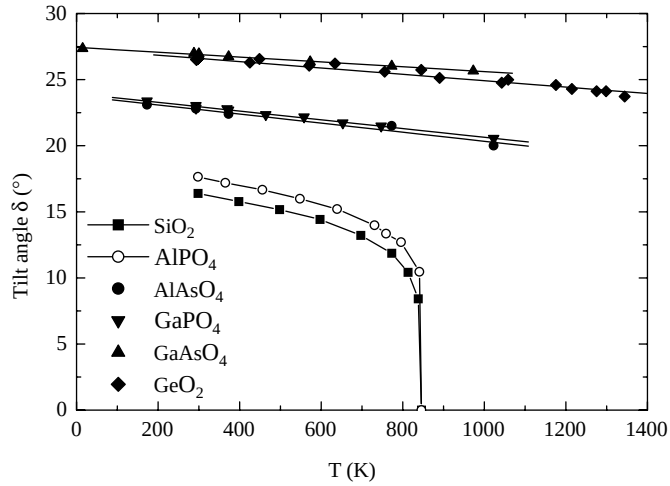

FIG. 5. Evolution of the tilt angle δ as a function of temperature for a series of α-quartz homeotypes. Data for SiO_2 (18), $AlPO_4$ (19), $AlAsO_4$ (20–22), $GaPO_4$ (20,21,23,24) and $GaAsO_4$ (3) are from the literature.

Phase Stability in GeO_2

The α-quartz-type form of GeO_2 is metastable with respect to the rutile-type form under ambient conditions. In the present experiments, the proportion of the rutile-type form was found to begin to increase significantly above about 1000 K and represented close to 30% of the total material at 1175 K (Table 1). This value increases only very slowly with time. This behavior has been observed in previous studies (7, 26) and was attributed to the slow kinetics of this transformation even at these high temperatures. This is probably true in the bulk material, but there may be an important surface effect, which causes the initial rapid increase in the amount of the rutile-type form. The present sample had a crystallite size of $\sim$80 nm and thus a

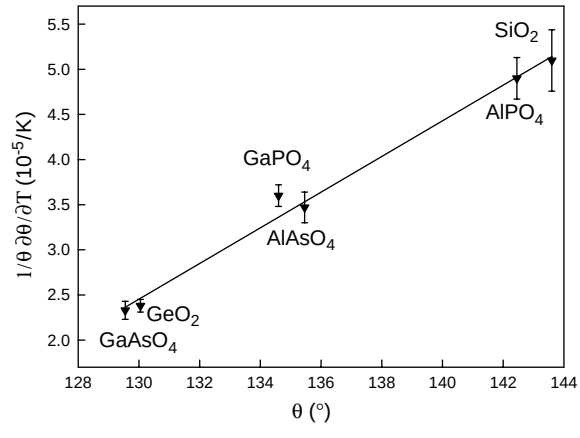

FIG. 6. Temperature dependence of the intertetrahedral bridging angle θ as a function of its room temperature value for a series of α-quartz homeotypes.

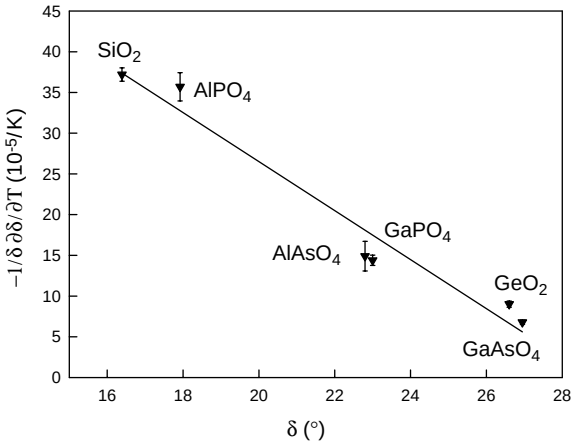

FIG. 7. Temperature dependence of the tilt angle δ as a function of its room temperature value for a series of α-quartz homeotypes.

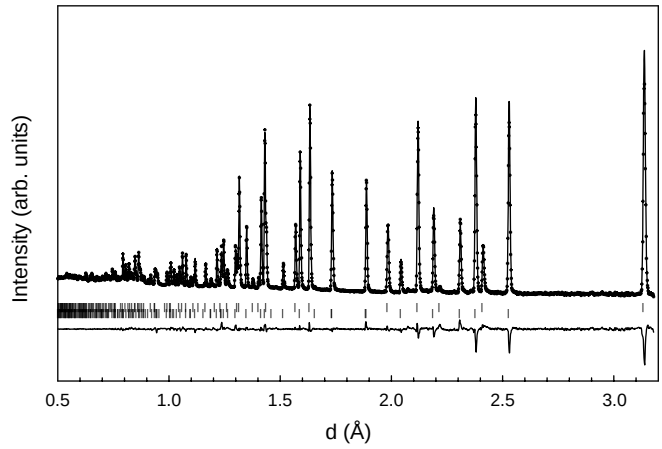

FIG. 8. Normalized experimental data (+), calculated and difference profiles (solid lines) from the Rietveld refinement of α-quartz-type GeO_2 at 1175 K using neutron diffraction data from Polaris. Intensity is in arbitrary units and the difference profile is on the same scale. The larger apparent differences between the normalized experimental and calculated intensities at higher d values are due to the lower counting statistics on these points due to the incident neutron flux. Vertical bars indicate the positions of all calculated reflections for the α-quartz-type phase (below) and the rutile-type phase (above).

large surface area. It is well known that pressure drives the transition to the rutile-type phase (27) and that the surface effect governed by grain size contributes to the internal pressure as given by the Laplace relationship. Surface defects such as OH groups may also play a role. Above 1320 K, the rutile-type material transformed to the α-quartz-type form, which is the stable phase in this temperature region up to the melting point. A cristobalite-type form of germanium dioxide is also known to exist, but it is always metastable (28). It can be noted that the α-quartz-type form of GeO_2 is stable at the highest temperatures for any α-quartz homeotype (1). All other known materials of this group transform or decompose at lower temperatures.

The refined structural data for the tetragonal, rutile-type phase at 1175 K (Table 6 and Fig. 8) indicate that the only free atomic positional parameter, the x-coordinate of oxygen, increases slightly with respect to the ambient temperature value of 0.30604 (29). Expansion along **a** is essentially twice that along **c** due to the larger relative increase in the apical Ge–O distances in the GeO_6 octahedron.

In the presence of water, the transition to the rutile-type phase can be found to occur as low as 465 K (9). The present study was performed under high vacuum on a very fine powder (crystallites of the order of 80 nm). The metastability of the α-quartz-type form will depend on grain size and the sample environment. It is probable that large single crystals will exhibit a larger domain of metastability than fine powders, which have a larger surface area and are more reactive. Germanium dioxide may thus be considered as a potential candidate for piezoelectric applications, but its use will probably be restricted to dry environments. In the presence of water, the transition to the rutile-type form will result in a loss of piezoelectric properties.

The α-quartz-type form of GeO_2 is also metastable at high pressure and room temperature. Transitions are observed above 6 GPa to polymorphs in which germanium is in six-fold coordination (11,30,31). Two distinct materials are obtained, either a monoclinic crystalline form (11,31) or an amorphous form (26,32,33). In contrast to the observed metastability at room temperature, moderate heating of the quartz-type form at, for example, 493 K and 3 GPa induces the phase transition to the stable rutile-type form (27).

TABLE 6
Cell Constants, Fractional Atomic Coordinates, Anisotropic Atomic Displacement Parameters (Å^2), and Octahedral Bond Distances for Rutile-Type GeO_2 at 1175 K

a= 4.43461(3) Å
c= 2.87308(3) Å
x = 0.3068(1)
Ge–O [2]: 1.9239(6) Å
Ge–O [4]: 1.8794(4) Å

	$100 \times U_{11}$	$100 \times U_{22}$	$100 \times U_{33}$	$100 \times U_{12}$
Ge	1.05(2)	1.05(2)	0.61(2)	−0.07(3)
O	1.47(2)	1.47(2)	0.92(3)	−0.49(3)

Note. Space group $P4_2/mnm$, $Z = 2$, Ge on 4*a* sites (0,0,0), O on 8*f* sites (x,x,0).

CONCLUSION

The present refinements of the structure of α-quartz-type germanium dioxide using neutron diffraction data indicate

that the high degree of structural distortion is retained up to the melting point. In particular, the temperature dependence of the intertetrahedral A–O–A' bridging angle, θ, and the tilt angle, δ, is lower than those of all α-quartz homeotypes, except for gallium arsenate. In this group of materials, this temperature dependence is found to be a function of the structural distortion. The present results indicate that α-quartz-type germanium dioxide is a potential candidate for piezoelectric applications at high temperature. Two obstacles remain to be overcome before this material can be used. Crystal growth of this metastable form must be optimized and problems related to the transformation to the stable rutile-type phase need to be addressed.

ACKNOWLEDGMENTS

We thank Simine Short for assistance with the experiment on SEPD. This work benefitted from the use of the Intense Pulsed Neutron Source of Argonne National Laboratory which is funded by the US Department of Energy, BES-Materials Science, under Contract W-31-109-ENG-38.

REFERENCES

1. E. Philippot, A. Goiffon, A. Ibanez, and M. Pintard, *J. Solid State Chem.* **110,** 356 (1994).
2. E. Philippot, D. Palmier, M. Pintard, and A. Goiffon, *J. Solid State Chem.* **123,** 1 (1996).
3. E. Philippot, P. Armand, P. Yot, O. Cambon, A. Goiffon, G. J. McIntyre, and P. Bordet, *J. Solid State Chem.* **146,** 114 (1999), doi:10.1006/jssc.1999.8316.
4. J. Haines, C. Chateau, J. M. Léger, and R. Marchand, *Ann. Chim. Sci. Mat.* **26,** 209 (2001).
5. J. Glinnemann, H. E. King Jr., H. Schulz, Th. Hahn, S. J. La Placa, and F. Dacol, *Z. Kristallogr.* **198,** 177 (1992).
6. R. A. Young, Defence Documentation Centre. Rep. No. AD 276, 235, Washington, DC, 1962.
7. A. W. Laubengayer and D. S. Morton, *J. Am. Chem. Soc.* **54,** 2303 (1932).
8. T. B. Kosova and L. N. Dem'yanets, Russ. *J. Inorg. Chem.* **33,** 2654 (1988).
9. D. V. Balitsky, V. S. Balitsky, Yu. V. Pisarevsky, E. Philippot, O. Yu. Silvestrova, and D. Yu. Pusharovsky, *Ann. Chim. Sci. Mat.* **26,** 183 (2001).
10. S. Hull, R. I. Smith, W. I. F. David, A. C. Hannon, J. C. Mayers, and R. Cywinski, *Physica B* **180/181,** 1000 (1992).
11. J. Haines, J. M. Léger, and C. Chateau, *Phys. Rev. B* **61,** 8701 (2000).
12. A. C. Larson and R. B. Von Dreele, in "GSAS: General Structure Analysis System." Los Alamos National Laboratory, Los Alamos NM, 1994.
13. M. G. Tucker, D. A. Keen, and M. T. Dove, *Mineral. Mag.* **65,** 489 (2001).
14. G. S. Smith and P. B. Isaacs, *Acta Crystallogr.* **17,** 842 (1964).
15. K. M. Murthy, *J. Am. Ceram. Soc.* **45,** 616 (1962).
16. Ph. Gillet, A. Le Cléac'h, and M. Madon, *J. Geophys. Res.* **95,** 21,635 (1990).
17. M. S. Ghiorso, I. S. E. Carmichael, and L. K. Moret, *Contrib. Mineral. Petrol.* **68,** 307 (1979).
18. K. Kihara, *Eur. J. Mineral.* **2,** 63 (1990).
19. Y. Maruoka and K. Kihara, *Phys. Chem. Miner.* **24,** 243 (1997).
20. A. Goiffon, J. C. Jumas, M. Maurin, and E. Philippot, *J. Solid State Chem.* **61,** 384 (1986).
21. A. Goiffon, G. Bayle, R. Astier, J. C. Jumas, M. Maurin, and E. Philippot, *Rev. Chim. Minér.* **20,** 338 (1983).
22. O. Baumgartner, M. Behmer, and A. Preisinger, *Z. Kristallogr.* **187,** 125 (1989).
23. O. Baumgartner, A. Preisinger, P. W. Krempl, and H. Mang, *Z. Kristallogr.* **168,** 83 (1984).
24. H. Nakae, K. Kihara, M. Okuno, and S. Hirano, *Z. Kristallogr.* **210,** 746 (1995).
25. H. Grimm and B. Dorner, *J. Phys. Chem. Solids* **36,** 407 (1975).
26. M. Madon, Ph. Gillet, Ch. Julien, and G. D. Price, *Phys. Chem. Miner.* **18,** 7 (1991).
27. T. Yamanaka, K. Sugiyama, and K. Ogata, *J. Appl. Crystallogr.* **25,** 11 (1992).
28. E. Hauser, H. Nowotny, and K. J. Seifert, *Monatsh. Chem.* **101,** 7 15 (1970).
29. A. A. Bolzan, C. Fong, B. J. Kennedy, and C. J. Howard, *J. Solid State Chem.* **113,** 9 (1994).
30. J. P. Itié, A. Polian, G. Calas, J. Petiau, A. Fontaine, and H. Tolentino, *Phys. Rev. Lett.* **63,** 398 (1989).
31. V. V. Brazhkin, E. V. Tat'yanin, A. G. Lyapin, S. V. Popova, O. B. Tsiok, and D. V. Balitskĭ, *JETP Lett.* **71,** 293 (2000).
32. T. Yamanaka, T. Shibata, S. Kawasaki, and S. Kume, in "High-Pressure Research: Applications to Earth and Planetary Sciences" (Y. Syono and M. H. Manghnani, Eds.), p. 493. Terra Scientific, Tokyo and American Geophysical Union, Washington, DC, 1992.
33. M. S. Somayazulu, N. Garg, S. M. Sharma, and S. K. Sikka, *Pramana* **43,** 1 (1994).